Evaluation of Variation in Source Parameters of Repeating Characeristic Subduction Earthquakes in Case of Characteristic Earthquakes off Kesennuma, northeast Japan

*Kimiyuki Asano[1]

1.Disaster Prevention Research Institute, Kyoto University

After the experience of the 2011 Tohoku earthquake, scenario-based strong motion prediction is strongly required quantitatively to show its variation or uncertainty. In this presentation, we focus on the variation or uncertainty of source parameters such as area and stress drop of strong motion generation area (SMGA). In the strong motion prediction recipe, outer and inner source parameters are given by the empirical scaling relationships (e.g., Murotani *et al.*, 2008). Each empirical scaling relationship has its standard deviation. However, such standard deviation is combination of variation due to difference in source characteristics among many different source regions and one due to the deviation among repeating events in a specific source region. In order to develop more sophisticated strong motion prediction, we would like to separate these two factors of variations from each other to obtain reasonable probabilistic distributions of source parameters by analyzing repeating characteristic earthquakes occurring in a same source region. Nagai *et al.* (2001) and Yamanaka and Kikuchi (2004) are pioneering studies for such objectives, however, what aspect of SMGA will be preserved and deviated is need to be investigated for advancing strong motion prediction framework. Particularly in northeast Japan, repeating characteristic subduction earthquakes have been observed during the history of strong motion observation. For example, Takiguchi *et al.* (2011) analyzed SMGAs for the 1982 and 2008 off Ibaraki earthquakes (both events are M_J7.0), and they concluded that the size of SMGA is same for two events, but the stress drop of SMGA for the 1982 event is 1.5 times larger than that of 2008 event.
In this study, repeating characteristic subduction earthquakes occurring off Kesennuma, northeast Japan, are analyzed. The latest event occurred on May 13, 2015 (M_J6.8). According to Hasegawa *et al.* (2005) and Takasai *et al.* (2014), M6-class events repeatedly occurred in 1940, 1954, 1973, 1986, and 2002. They showed that the average repeating period is 15.5 years and the average JMA magnitude is 6.3. Two events occurring in 2002 and 2015 are densely observed by K-NET and KiK-net operated by NIED. PARI continues strong motion observation in many ports over 50 years, and four events (1974, 1986, 2002, and 2015) were observed by their network. The figure below shows comparison of the EW components of observed velocities in 0.2–2 Hz at Ofunato-Bochi station of PARI. The pulse length of the direct S-wave is almost same for these four events, but the maximum amplitude of the 2015 event is largest among the four events. From above comparison, the size of SMGA for these four events might be almost equivalent to each other, and the difference in the waveforms reflects the difference in stress drop of SMGA. We will further discuss on the variation in stress drop based on the spectral ratio method and waveform modeling.
Acknowledgements: The strong motion data from K-NET, KiK-net (NIED) and PARI are used in this study.

Keywords: Repeating characteristic earthquakes, Source characteristics, Strong motion generation area

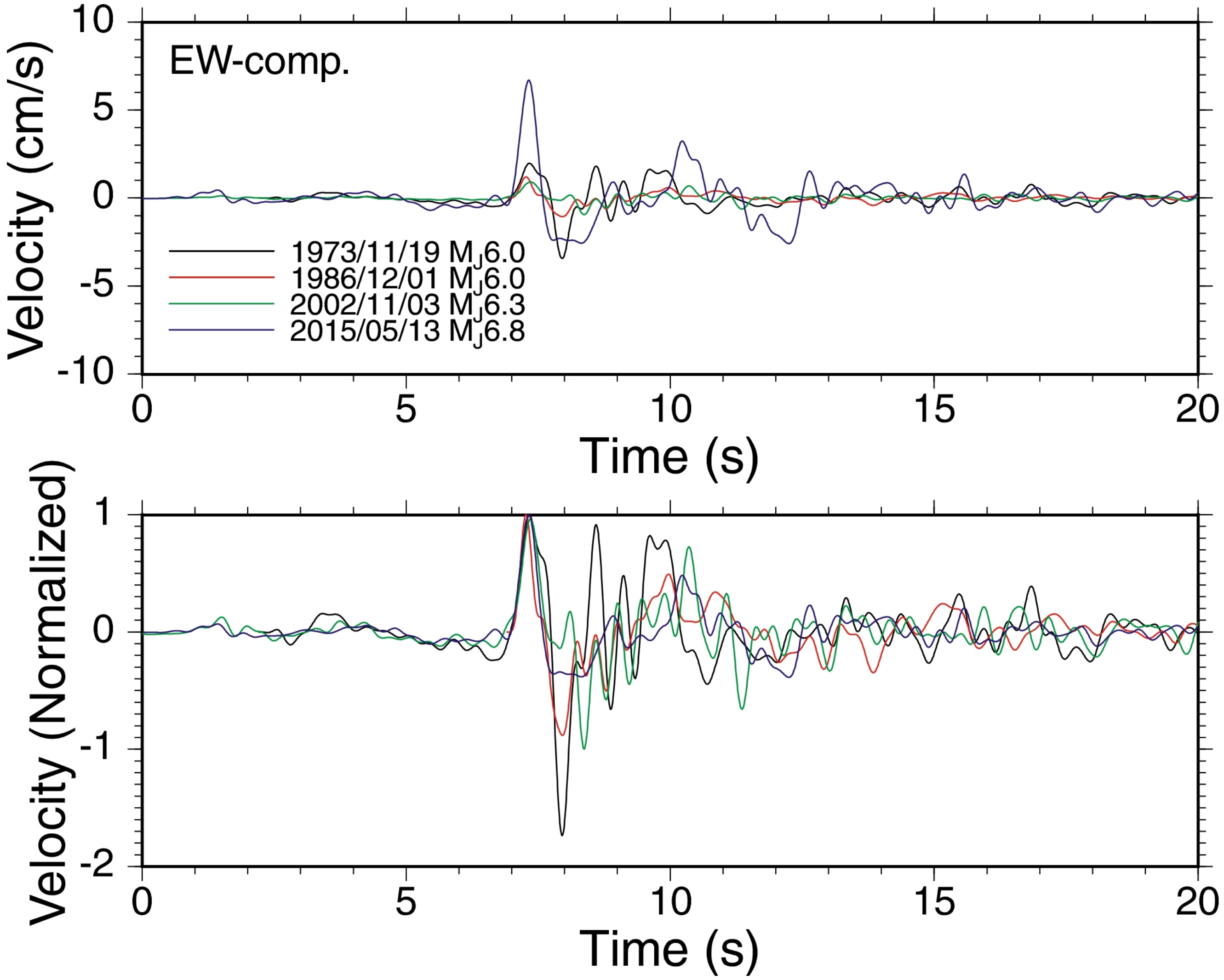
EW-comp.
Velocity (cm/s)
10
5
0
-5
-10
1973/11/19 MJ6.0
1986/12/01 MJ6.0
2002/11/03 MJ6.3
2015/05/13 MJ6.8
0
5
10
15
20
Time (s)
Velocity (Normalized)
1
0
-1
-2
0
5
10
15
20
Time (s)

A study on effects of uncertainty in fault width to strong motion evaluation for earthquakes in active faults

*Nobuyuki Morikawa[1], Takahiro Maeda[1], Asako Iwaki[1], Hiroyuki Fujiwara[1]

1.National Research Institute for Earth Science and Disaster Prevention

The lower-depth of the seismogenic zone is estimated from hypocenter distribution of small earthquakes in the long-term evaluation of earthquakes in active faults by Earthquake Research Committee of Japan (ERCJ), but there is a possibility that the fault bottom becomes deeper than that when a large earthquake occurs. However, almost no knowledge how deep it is. Therefore the consideration of epistemic uncertainty in the lower-depth of the seismogenic zone, the fault width, is required in the strong-motion evaluation.
The magnitude of an earthquake changes with the fault width by using the method (A) of strong motion evaluation method “recipe” by ERCJ. On the other hand, the magnitude of an earthquake is determined from the fault length by using the method (B) of the "recipe". Therefore the magnitude of an earthquake does not change with the fault width, but the values of source parameters, such as slip and static stress drip, change because the relation between seismic moment and fault area vary in this case.
As mentioned above, dependence of fault width on outer- and inner-source parameters determined from the “recipe” is very complicated. In this study we examine calculations of strong ground motion for some models considering uncertainty of the lower depth of the seismogenic zone and compare the results. It is also necessary to consider the uncertainty in dip angle of the fault as the parameter related to the fault width, but we consider only uncertainty in the lower-depth of the seismogenic zone here.

Keywords: Uncertainty, Strong ground motion, Fault width, Active faults

Construction of a recipe for predicting strong ground motions from subduction mega-thrust earthquakes

*Kojiro Irikura[1], Susumu Kurahashi[1]

1.Aichi Institute of Technology

Introduction
Before the 2011 Mw 9 Tohoku earthquake, there are considered six segments for the region off the coast of Tohoku from Middle Sanriku-Oki to Ibaragi-Oki with seismic activities of past 400 years by the Headquarter of Earthquake Research Promotion, Japan (HERP). Then, they made a long-term forecast that Mw 7–8.4 earthquakes would occur within those segments, having different recurrence times from one to the other. Prior to the Mw 9 event, the possibility of a megathrust earthquake of magnitude larger than 8.5 was never expected from a scientific point of view. On the other hand, we find the segmentation might control the characteristics of ground motions from the rupture process inversion of near-field strong motion records as well as earthquake occurrence in the source region of this event. Then, we propose an improved idea for recipe of predicting strong ground motions for subduction earthquakes.
Segmentation
There were not only along-strike segments but also along-dip ones for the source region of the Mw 9 event. The high frequency radiation is dominated from SMGAs in segments located in a down-dip region closer to Japan coast similar to high-frequency backprojection studies using teleseismic short-period P waves data. The low frequency radiation from the asperity inverted from long-period strong-motions data tends to dominate in the shallow segment closer to the trench. Similarly, apparent along-dip rupture differences were observed for several other large megathrust events such as the 2010 Mw 8.8 Maule earthquake in Chile, the 2005 Mw 8.6 Sumatra earthquake, and the 2004 Mw 9.2 Sumatra earthquake by comparing the slip distribution with HF radiation observations (Yao et al., 2015).
Short-period Source model
From the observed strong motions during the Tohoku event, there are recognized distinctive five wavepackets that correspond to ground motions from respective small asperities. The origins of the wavepackets were retrieved from data arrays consisting of the strong motion stations using a semblance analysis. Then, we estimate a short-period source model for generating strong ground motions from this earthquake by comparing the observed records from the mainshock with synthesized motions based on a multiple-asperity source model and the empirical Green’s function method. We find that five small-asperities in the down-dip areas generate short-period motions of engineering interest but large asperities in the shallower area east of hypocenter generate mainly large slip and long-period ground motions. We call such small asperity strong-motion generation area (SMGA). This model provides broadband ground motions including long-period motions from 2 s to 10 s that are engineering interest for aseismic design and base-isolation.
Impulsive waves from SMGA
Another problem is that the short-period source models with such SMGAs cannot simulate impulsive waves with high acceleration and velocity seen at onsets of the wave-packets in strong motion records observed near the source fault. To generate such impulsive waves, multi-scale source model is needed with heterogeneity of maximum slip velocity and rise time inside the SMGAs. Then the recipe of predicting broadband ground motions from 0.1 s to 10 s for mega-thrust subduction earthquakes is needed to consider the multi-scale heterogeneous model.

Keywords: subduction mega-thrust earthquakes, strong ground motions, short-period source model, strong motion prediction recipe

Near-field strong motion on the hanging wall of low angle thrusting: a case of Hamaoka

*Ichiro Kawasaki[1]

1.Tono Research Institute of Earthquake Science, Association for the Development of Earthquake Prediction

(1) We discuss the near-filed strong motion at Hamaoka on hanging wall of low angle thrusting. The key parameter is slip velocity.
(2) The high stress drop of 22 MPa has raised a problem on the evaluation of near-field strong motion. As fas as ever documented in Japan, stress drops of subduction zone earthquakes and average slip velocities were estimated to be around 3-5 MPa and 1 m/s, respectively. Following Starr (1928) for dip slip faulting, a stress drop Δσis proportional to Do/W, where Do is an average slip and W is a fault width. Following Brune (1970) and Ida and Aki (1972), an average slip velocity Do/to is proportional to earthquake generating stress σe, where to is a risetime. Assuming that σe is the same as Δσ, both Do and Do/to are proportional to σe, leading to the recognition that velocity and acceleration amplitude of synthetic strong motion are proportional to σe in the near-field to the first order.
(3) We move to a discussion of strong motion at Hamaoka. Assuming fault parameters as a fault length 100 km, W 50 km, and bilateral propagation in strike-parallel direction and unilateral propagation upward of rupture front from the center of the lower side, we obtain synthetic strong motion (Fig.1) at Hamaoka for three cases of Do/to of 1 m/s, 3 m/s and 5 m/s with a common Do of 15 m. Numerical computation is done by programs of Kawasaki et al. (1973) and Okada (1980). Velocity and acceleration are roughly proportional to Do/to. When Do/to is larger than 3 m/s, the maximum amplitude of acceleration is larger than g.
(4) We can not apply above discussion to shorter period strong motion because far-field term gets relatively predominant and physical attenuation and scattering become effective. However, on the following assumptions (a) and (b)
(a) velocity and acceleration of strong motion are proportional to slip velocity and earthquake generating stress in every scales of multi-scale rupturing phenomena,
(b) stress level of level 2 megathrust earthquake would be far higher than those of level 1 subduction zone earthquakes,
we can postulate that strong motions at Hamaoka during the coming level 2 class Mw9 Nankai trough earthquake would be far larger than those during level 1 class 1944 Tonankai and 1854 Ansei-Tokai earthquakes.
(5) Thus, reliable evaluation of near-field strong motion on the hanging wall of low angle thrusting seems to be not feasible at the present stage of seismology. The evaluation of regional tectonic stress on the hanging wall and the distribution of the strong asperity on the subduction interface are indispensable.
(6) Figure caption
Fig.1 Synthetic strong motions at Hamaoka for three cases of slip velocities of 1 m/s, 3 m/s and 5 m/s with a common slip Do of 15 m. Other fault parameters are given in the text. Left, middle and right panels are displacement (U), velocity (V) and acceleration (A), respectively. Upper and lower raw panels are those of fault perpendicular motion (subscript x) and vertical motion (z), respectively. A distance from Hamaoka to subduction interface is 10 km.

Keywords: near-field, low angle thrusting, earthquake generating stress, slip velocity, strong motion, Hamaoka

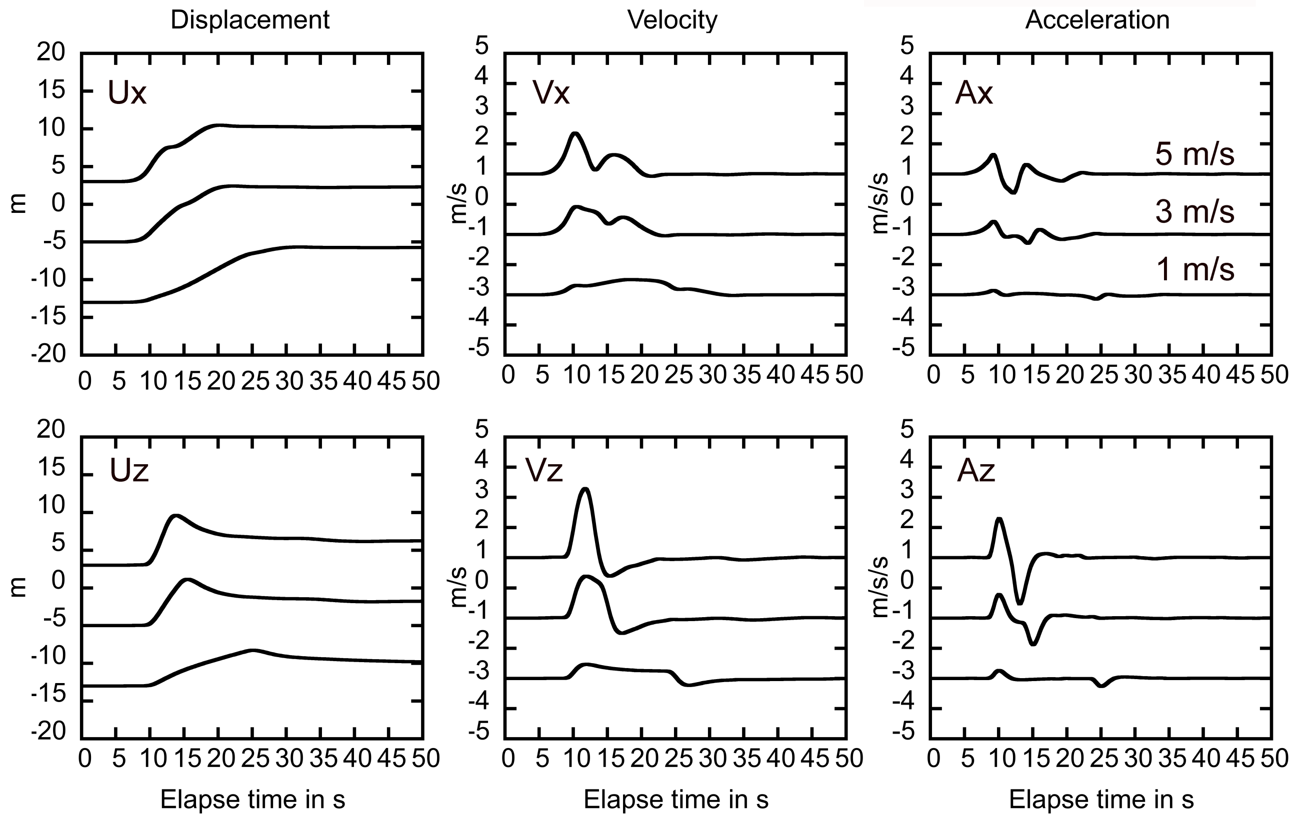
Displacement
Velocity
Acceleration
Ux
Vx
Ax
Uz
Vz
Az
5 m/s
3 m/s
1 m/s
m
m/s
m/s/s
Elapse time in s
Elapse time in s
Elapse time in s

Long-period ground motion evaluation for the Sagami Trough megathrust earthquakes

*Takahiro Maeda[1], Asako Iwaki[1], Nobuyuki Morikawa[1], Ryuta Imai[2], Shin Aoi[1], Hiroyuki Fujiwara[1]

1.National Research Institute for Earth Science and Disaster Prevention, 2.Mizuho Information & Research Institute, Inc.

We evaluate long-period ground motions associated with the Sagami Trough earthquakes, especially for the 1703 Genroku earthquake and the 1923 Taisho earthquake. The long-period ground motions are simulated by the finite difference method using a characterized source model and the 3-D velocity structure model. The parameters of the characterized source model are determined based on a “recipe” for predicting strong ground motion [Earthquake Research Committee (ERC), 2009]. We construct 408 source models for hypothetical Genroku and Taisho earthquakes assuming possible source parameters, including asperity configuration, asperity size and hypocenter location (120 models and 288 models for hypothetical Taisho and Genroku earthquakes, respectively). And then we introduce a multi-scale heterogeneity (Sekiguchi and Yoshimi, 2006) of rupture propagation (rupture velocity, slip, rake angle) to the characterized source models. The 3-D velocity structure model used in the simulation is a recently constructing model for the Kanto area (Senna et al., 2015, SSJ). Using these models, an analyzing period range of our simulation is >2 s.

We use peak ground velocity (PGV) and velocity response spectra (Sv) as indices for the evaluation. Spatial distribution maps of PGV and Sv indicate that the hypocenter location has larger impact on the distribution. Because the source areas are located beneath the Kanto plane, body waves predominate in simulated waveforms for station in the plane. Histograms of PGV and Sv show a log-normal like distribution. Using these results, we evaluate the long-period ground motion hazard for two types of Kanto earthquake.

This study was supported by the Support Program for Long-Period Ground Motion Hazard Maps by the Ministry of Education, Culture, Sports, Science and Technology (MEXT).

Keywords: Sagami Trough, Long-period ground motion, Finite difference method

The long-period ground motion between P and S arrivals observed by the deep borehole strainmeters and stressmeters

*Osamu Murakami[1], Hiroshi Ishii[1], Yasuhiro Asai[1]

1.Tono Rearch Institute of Earthquake Science, Association for the Development of Earthquake Prediction

We deployed multi-component borehole instruments equipped with strainmeters and/or stressmeters around the Tono Research Institute of Earthquake Science (TRIES). We recorded the continuous data at a rate of 1-50 Hz for these instruments. In these records, we observed the long-period variations between P and S arrivals from large earthquakes. In order to investigate the nature of these long-period variations, we estimated the dominant periods of these variations. After we manually picked the P and S wave arrivals for each waveform, we calculated spectrum of the records between P and S wave arrivals. We found that the dominant periods of these long-period variations are typically a few tens seconds. Though W phase (Kanamori, 1993) is well known as the long-period phase between P and S arrivals, the periods of W phase are usually hundreds seconds or more, and are longer than our observed dominant periods. We consider that the observed long-period variations are responsible for other effects, such as PL wave caused by the leaking mode (Yoshii, 1970). These long-periods variations are also recorded by seismometers equipped with the same borehole instruments installed in deep borehole. The long-periods variations observed at seismometers, however, will be clearly found, after we applied the bandpass (0.01 -0.1 Hz) filter. Because the strainmeters and stressmeters have enough sensitivity to DC, we consider that the strainmeters and stressmeters are also useful to detect the long-period ground motions. We will present the results obtained from the analysis.

Keywords: long-period ground motion between P and S arrivals, strainmeters, stressmeters, borehole

Studying the effect of seawater on seafloor strong ground motions using simulation method

*Hongqi Diao[1,2], Jinjun Hu[2], Lili Xie[2,3]

1.Earthquake Research Institute, The University of Tokyo, Tokyo 113-0032, Japan, 2.Key Laboratory of Earthquake Engineering and Engineering Vibration, Institute of Engineering Mechanics, China Earthquake Administration, Harbin 150080, China, 3.School of Civil Engineering and Architecture, Harbin Institute of Technology, Harbin 150090, China

For the seismic design of offshore engineering, we need to estimate the design parameters of seafloor strong motion. Under the influence of seawater and seafloor soil, seafloor ground motion may present different characteristic from that of onshore ground motion. Until now, there have been very few researches on the seafloor strong motion and also very little seafloor strong motion data has been observed. Our present paper focuses on the effect of seawater on the engineering characteristics and attenuation characteristic of seafloor strong motion. Our main work includes two main parts: one is the effect on engineering characteristics (PGA, Fourier spectra and acceleration response spectra, and 90% energy duration)of seafloor strong motion under seawater of different depth; and the other is the effect of seawater for 50-meter depth on seafloor strong motion attenuation characteristic. Using the wavenumber integration method program of Computer Programs in Seismology (CPS), we perform numerical simulation of seafloor ground motions in six different conditions(water depth: 50 meter, 60 meter, 70 meter, 80 meter, 90 meter and 100 meter) for three kinds of fault types(Normal fault, Reverse fault and Strike-slip fault) and compare them with that without seawater on them. As a result, for whatever kind of fault types, the difference of effect on seafloor horizontal ground motions of seawater is little and can be ignored. However, the effect on seafloor vertical ground motions of seawater is obvious. For all the three kinds of fault types, with the increasing depth of seawater, the effects on vertical motions are similar: 1) waveform becomes more visually complicated; 2) PGA becomes smaller; 3) Fourier spectra decreases greatly near the P wave resonance frequencies of seawater, acceleration response spectra becomes smaller in short periods less than 0.1s. The effect on 90% energy duration time of seafloor vertical motion of seawater has something to do with fault types. We establish the attenuation characteristic relationships of PGA and acceleration response spectra for seafloor vertical ground motion with 50-meter depth of seawater using CPS software and compare them with that without seawater. We found that: the 50-meter depth of seawater has a great effect on the attenuation relationships of PGA and the acceleration response spectra in very short periods (not exceeding 0.04s), the PGA and acceleration response spectra values of seafloor vertical motion are obviously smaller than those without water.

Keywords: seawater, seafloor ground motion, numerical simulation, attenuation characteristic relationship

Finite Source Modeling of a Large Earthquake Using the Ambient Seismic Field

*Loic Viens[1], Hiroe Miyake[2,1], Kazuki Koketsu[1]

1.Earthquake Research Institute, University of Tokyo, 2.Center for Integrated Disaster Information Research, Interfaculty Initiative in Information Studies, University of Tokyo, Tokyo, Japan

Large (M_w ≥7) earthquakes have the potential to generate long-period seismic waves that can be significantly amplified, even at large distances, by sedimentary basins. Prediction of these long-period ground motions (≥4 s) is essential to mitigate their impact on large-scale structures, such as high-rise buildings and oil storage tanks. We focus on the well-recorded Iwate-Miyagi Nairiku earthquake (M_w 6.9), which occurred on 14 June 2008 in the Tohoku region, Japan. This earthquake, which has a reverse-fault mechanism, caused several fatalities, collapse of houses and a bridge, and severe landslides. To simulate the long-period ground motions (4-10 s) generated by this event, we take advantage of the ambient seismic field continuously recorded by seismic stations of the Hi-net/NIED, Japan Meteorological Agency, and Tohoku University networks. Stations located in the vicinity of the mainshock fault plane are used as virtual sources and other stations as receivers. We use the deconvolution method to extract single force impulse response functions between each pair of stations. We first show that, after calibration of the amplitude, impulse response functions accurately simulate the long-period ground motions of a moderate M_w 5.0 aftershock that occurred close to the mainshock hypocenter. To simulate the mainshock, we construct a simple finite source model that is similar to the ones determined by source inversions. The fault plane is first discretized into subfaults of the size of the moderate M_w 5.0 earthquake. We show that it is possible to interpolate the impulse response functions extracted between every virtual source and each receiver to obtain one impulse response function for each subfault. We finally initiate and spread the rupture radially from the hypocenter with a constant velocity to simulate the long-period ground motions. We find that the simulated long-period ground motions are consistent with the earthquake records, which confirm the power of this technique to assess seismic hazard.

Keywords: Ground motion simulation, Ambient seismic field, Green's function, Finite source modeling

Estimation of site amplifications for strong motion stations in Hokuriku district, Japan, based on spectral inversion technique

*Kazuhiro Somei[1], Kimiyuki Asano[2], Tomotaka Iwata[2], Ken Miyakoshi[1], Michihiro Ohori[3]

1.Geo-Research Institute, 2.Disaster Prevention Research Institute, Kyoto University, 3.Research Institute of Nuclear Engineering, University of Fukui

To develop the underground velocity structure model for strong motion prediction in Hokuriku district (i.e., Fukui, Ishikawa, and Toyama prefectures), Japan, we evaluate site amplification factors for strong motion stations in this area. Strong motion stations targeted in this study are K-NET, KiK-net, and F-net operated by the National Research Institute for Earth Science and Disaster Prevention (NIED), Japan, and local government Shindo-kei networks in Fukui, Ishikawa, and Toyama prefectures. Owing to dense strong motion stations including local government Shindo-kei networks, we can obtain high density local site amplification factors, especially for the urbanized area, in Hokuriku district.

Site amplifications are estimated by separating source, propagation path, and site characteristics from observed Fourier amplitude spectra based on the spectral inversion technique. We use the vectorial summation of the two horizontal components of Fourier amplitude spectra, which are calculated from the windows of 10.24 s for S-wave records. A moving average of ±5 % window for each frequency point is applied to smooth the amplitude spectra. We choose the F-net SRN station as a reference rock site assuming no site amplification to resolve the trade-off between the source spectra and site effect.

For example of K-NET ISK011, the site amplification from spectral inversion shows the peak between 0.5 and 2.0 Hz with amplification factor from 10 to 20. On the other hand, the 1-D theoretical amplification factor based on the velocity structure model by Japan Seismic Hazard Information Station does not show the peak between 0.5 and 2.0 Hz. However, the 1-D theoretical amplification factor calculated from the improved velocity structure model by using microtremor observations (Asano et al., J. Jpn. Assoc. Earthq. Eng., 15(7), 194-204, 2015) is from 10 to 20 between 0.5 and 2.0 Hz as well as the amplification from spectral inversion. Thus, the obtained high density site amplifications could be useful for performance-checking of existing velocity structure model for each local site, especially for the urbanized area. We identified where we need to improve the velocity structure model by comparing the site amplification obtained from spectral inversion with 1-D theoretical amplification factor from existing velocity structure model in Hokuriku district.

Acknowledgements: Strong motion data of K-NET, KiK-net, and F-net provided by NIED are used in this study. We also use the strong motion data from local government Shindo-kei networks operated by Fukui, Ishikawa and Toyama prefectures, Japan. We thank to the staff in these institutes for maintaining and providing the observed records. This study was supported by the Special Project "Integrated Research Project on Seismic and Tsunami Hazards around the Sea of Japan" from the Ministry of Education, Culture, Sports, Science, and Technology of Japan.

Keywords: Site amplification, Hokuriku district, Spectral inversion, Strong motion station

Simulation of characteristic late arrivals after S-wave of local events between Amagasaki and Higashinada in Osaka sedimentary basin

Hiroki Tanaka[1], *Tomotaka Iwata[1], Kimiyuki Asano[1]

1.Disaster Prevention Research Institute, Kyoto University

Tanaka et al.(2014,2015, SSJ fall meeting) analyzed distinctive later arrivals after direct S-waves of local events at Amagasaki strong motion station (CEORKA), and at Ashiya, Fukuike, and Fukae temporary strong motion stations (Iwata et al., 1995). They found that the polarization angles and the linearity of those phases changed systematically with according to the number of reverberations at Amagasaki station, whereas there are not significant phases appeared at other three stations. Those findings suggest that the three-dimensional basin velocity structure affects the reverberation characteristics.
To confirm the observation characteristics, we then conducted the three-dimensional ground motion simulations up to 2Hz using a three-dimensional basin velocity structure model (Sekiguchi et al., 2013) and a double-couple point source model. The simulation reproduces the observation well and proved that those systematic characteristics of the distinctive later phases are caused by the three-dimensional shape of the basin/bedrock interface. From the simulation results, the Amagasaki station locates in the area where the distinctive late phases can be observed clearly. On the contrary, other three stations locates in the area where the S-wave reverberations and the basin-induced surface waves appear simultaneously so as to contaminate clear arrivals.

Keywords: Osaka sedimentary basin velocity structure model, ground motion simulation, multiple-reflection

Strong-motion simulation of the 2015 Southern Oita, Japan, earthquake (Mj5.7) using a 3D structure model including the land and sea-floor topography

Tatsuya Okunaka[2], Masanao Komatsu[1], *Hiroshi Takenaka[1], Masayuki Yoshimi[3], Takeshi Nakamura[4], Taro Okamoto[5]

1.Department of Earth Sciences, Graduate School of Natural Science and Technology, Okayama University, 2.Department of Earth Sciences, Faculty of Science, Okayama University, 3.Geological Survey of Japan, AIST, 4.Japan Agency for Marine-Earth Science and Technology, 5.Department of Earth and Planetary Sciences, School of Science, Tokyo Institute of Technology

Oita prefecture is located in northeastern part of Kyushu Island which is characterized by active subduction of the Philippine Sea plate (PHS) beneath the Eurasian plate and several active volcanoes along with the volcanic front. Oita area has frequently been damaged by large earthquakes and tsunamis since ancient times. From the point of view of disaster prevention, it is important to improve the precision of strong ground motion prediction. In this study we construct a three-dimensional (3D) numerical structure model for simulation of the strong ground motion around Oita prefecture, which includes land and sea-floor topography and a seawater layer as well as subsurface structures of the arc side and the PHS slab, partially based on the J-SHIS model for near-surface structure (National Research Institute for Earth Science and Disaster Prevention) and the Integrated Velocity Structure Model for the arc crust and the slab-top depth model of the PHS (Headquarters for Earthquake Research Promotion, Japan). We then conduct the finite-difference-method (FDM) numerical simulations of strong motion for the 2015 Southern Oita, Japan, earthquake (Mj5.7) whose JMA hypocenter is located in the PHS slab mantle as well as the NIED F-net centroid and which has a strike-slip focal mechanism. We employ the Heterogeneity, Oceanic Layer, and Topography (HOT)-FDM scheme developed by Nakamura et al. (2012, BSSA) to simulate seismic wave propagation in land and ocean areas. From these simulations the best point source is found to be located in the PHS crust, not in the mantle, at depth of about 48 km which is shallower than the JMA hypocentral depth by 10 km. The simulated long-period (2-20 s) motions reproducing observed records demonstrate substantial contributions of thick low-velocity sediment layers in and around Beppu Bay and Oita basin to development of these motions. We also examine the topographic effects on the strong motion by analyzing these simulation results.

Keywords: strong motion, Oita, the 2015 Southern Oita, Japan, earthquake , long-period ground motion, simulation, finite-difference method

Modeling of the subsurface structure from the seismic bedrock to the ground surface for a broadband strong motion evaluation in Kanto area

*Shigeki Senna[1], Atsushi Wakai[1], Kaoru Jin[1], Takahiro Maeda[1], Katsumi Kimura[1], Hisanori Matsuyama[2], Hiroyuki Fujiwara[1]

1.National Research Institute for Earth Science and Disaster Prevention, 2.OYO Corp

Sophisticated predictions of strong ground motion are vital when constructing structure models that enable us to evaluate broadband ground motion features. Such models should integrate subsurface structure models for strata shallower than engineering bedrock and deep structure models for strata even deeper. Both such models used to be separately modeled separately so that observation data could be reproduced. In this study, we have created a subsurface structure model applicable from seismic bedrock to ground surface" for whole Kanto area, in attempts to sophisticate subsurface structure models.

We have ever collected bore-hole data and soil physical properties data, and then, by using them, have constructed initial geological models of subsurface structure from seismic bedrocks to ground surfaces in some areas of Japan, which have thicker sedimentary layers.

At present, we are constructing models of subsurface structure in wide area for Kanto and Tokai region of Japan as part of the national project, "Reinforcement of resilient function for disaster prevention and mitigation."

In this study, at first, we collected as many records as possible obtained by microtremor and earthquake observation in the whole Kanto area, including Tokyo. And then, using geological models based on the results of boring surveys as reference, subsurface structure model from seismic bedrock to ground surface was improved based on records of microtremor array and earthquake observation in those areas.

Keywords: strong ground motion evaluation, underground structure models, microtremor observation

ESTIMATION OF SEISMIC HAZARD FOR STRONG EARTHQUAKES IN TAIWAN

*YU-WEN CHANG[1]

1.NCREE National Center for Research on Earthquake Engineering of Taiwan

Two main factors that affect the result of ground motion prediction analysis are the existence of the event and site effect. A hybrid procedure, which combines site-dependent ground motion prediction and the limited real time observations, was set up to provide a high-resolution shakemap in a near-real-time manner after damaging earthquakes in Taiwan. The purpose of this paper is to develop the prediction model and procedure considering the characteristic of the damaging earthquake and local site effect, in order to provide an early estimation of potential hazard. In the site-dependent ground motion prediction model, the site effects of each strong motion stations are discussed in terms of a bias function that is site and intensity-level dependent function. Instead of such model, an empirical procedure is supplied to correct the discrepancy of the ground shaking estimated from the attenuation relation and applied to precisely estimate the shakemap of damaging earthquakes for emergency response.

Keywords: shakemap, site effect, ground motion prediction

Strong motion pulse and building collapse during the 2016 Tainan earthquake

*Kazuki Koketsu[1], Hiroaki Kobayashi[1], Hongjun Si[1], Loic Viens[1], Hongqi Diao[1], Hiroe Miyake[2]

1.Earthquake Research Institute, University of Tokyo, 2.Interfaculty Initiative in Information Studies, University of Tokyo

Ground motions during the 2016 Tainan earthquake have been observed by many stations of P-alert, which is an earthquake early warning system in Taiwan. Looking at the velocity seismograms at stations in Tainan City, a large long-period pulse is found mainly in the EW component to be as large as 100 cm/s at maximum. The Fourier spectrum of the seismogram at the station W21B indicates that the predominant period of this pulse was 1 to 4 s. The collapsed building causing more than 100 fatalities had 16 stories so that its natural period should be 0.8 to 1.3 s according to the relationship of natural period T and number of story N: T = (0.049 ~ 0.082)×N (Architectural Institute of Japan, 2000). Since the natural period can be longer due to construction defect, this pulse would have had a significant impact on the building.A source inversion of teleseismic body waves revealed that the source fault dipping to the north was located in the east of the city center of Tainan and a rupture consisting of strike-slip and reverse faulting propagated along the strike of the source fault. The westward rupture propagation towards the city center of Tainan went through parts of larger strike slip in the source fault. For a strike-slip fault, it is well known that the rupture directivity effect generates a long-period strong motion pulse in the direction perpendicular to the fault strike. However, the pulse of the Tainan earthquake was dominant in the EW direction, which was parallel to the fault strike. Therefore, a second source fault should be introduced around the area of aftershocks, or the geometry of the original source fault should be revised.

Keywords: Tainan earthquake, strong motion pulse, building collapse

Simulation of strong ground motions for the 1995 Kobe earthquake based on the pseudo point-source model

*Atsushi Nozu[1]

1.Port and Airport Research Institute

In our country, the characterized source model, which is composed of rectangular subevents generating strong ground motions, have extensively been used for the purpose of predicting strong ground motions (e.g., Kamae and Irikura, 1997). On the other hand, the author (Nozu, 2012) proposed a new source model, namely, the pseudo point-source model. In the model, the spaciotemporal distribution of slip within a subevent is not modeled. Instead, the source spectrum associated with the rupture of a subevent is modeled and it is assumed to follow the omega-square model (Aki, 1967). The source model consists of only six parameters for each subevent, namely, the longitude, latitude, depth, rupture time, seismic moment and corner frequency of the subevent. The model involves much less model parameters than the conventional characterized source model. Once the model parameters are given, by multiplying the source spectrum with the path effect and the site amplification factor, the Fourier amplitude at the site of interest can be obtained. Then, combining it with the Fourier phase of a smaller event, the time history of strong ground motions from the subevent can be calculated. Finally, by summing up contributions from the subevents, strong ground motions from the entire rupture can be obtained.
According to the results of past studies, the model can explain strong ground motions from a mega-thrust earthquake (Nozu, 2012) and an intraslub earthquake (Nagasaka et al., 2014), sometimes better than the conventional characterized source models. Its applicability to short distances, however, could be restricted, because it is expressing the subevent with a point. In addition, the current version of the pseudo point-source model does not consider directivity effects. Therefore, its applicability to shallow crustal earthquakes should carefully be examined by using observed records.
In this study, a pseudo point-source model with three subevents was developed for the Kobe earthquake and strong ground motions were simulated based on the model. According to the results, the pseudo point-source model can explain strong ground motions at KBU and MOT located in Kobe fairly well.
It is well known that strong ground motions in Kobe during the Kobe earthquake were affected by forward directivity (e.g., Kamae and Irikura, 1997). Then the question is why a pseudo point-source model, which does not consider rupture propagation explicitly, can explain strong motions in Kobe. To understand the reason, both Fourier amplitude and phase characteristics of the synthetic ground motions have to be considered. In terms of the Fourier amplitude, rupture propagation theoretically causes a shift in the corner frequency; the corner frequency is increased when the site is affected by forward directivity. In the present pseudo point-source model for the 1995 event, the corner frequencies were determined to be consistent with the observations and, as a result, the selected values of corner frequencies involve any effect of forward directivity. This should be one reason why the model can explain strong ground motions in Kobe. In terms of the Fourier phase, in general, the observed Fourier phase is the sum of the source, path and site effects. In the pseudo point-source model, because the Fourier phase of a small event is used, only the path and site effects are considered. This is equivalent to assuming that the source time function of each subevent is a delta function. Therefore, as long as the Fourier phase is concerned, the pseudo point-source model is actually suitable for the forward sites where the apparent source time function approaches to a delta function. It means that discrepancy is anticipated for the backward

sites. This point should be further studied using records from other crustal earthquakes with better azimuthal coverage.
Acknowledgement: Strong motion data used in this study were observed by the CEORKA.

Keywords: pseudo point-source model, the 1995 Kobe earthquake, strong ground motion

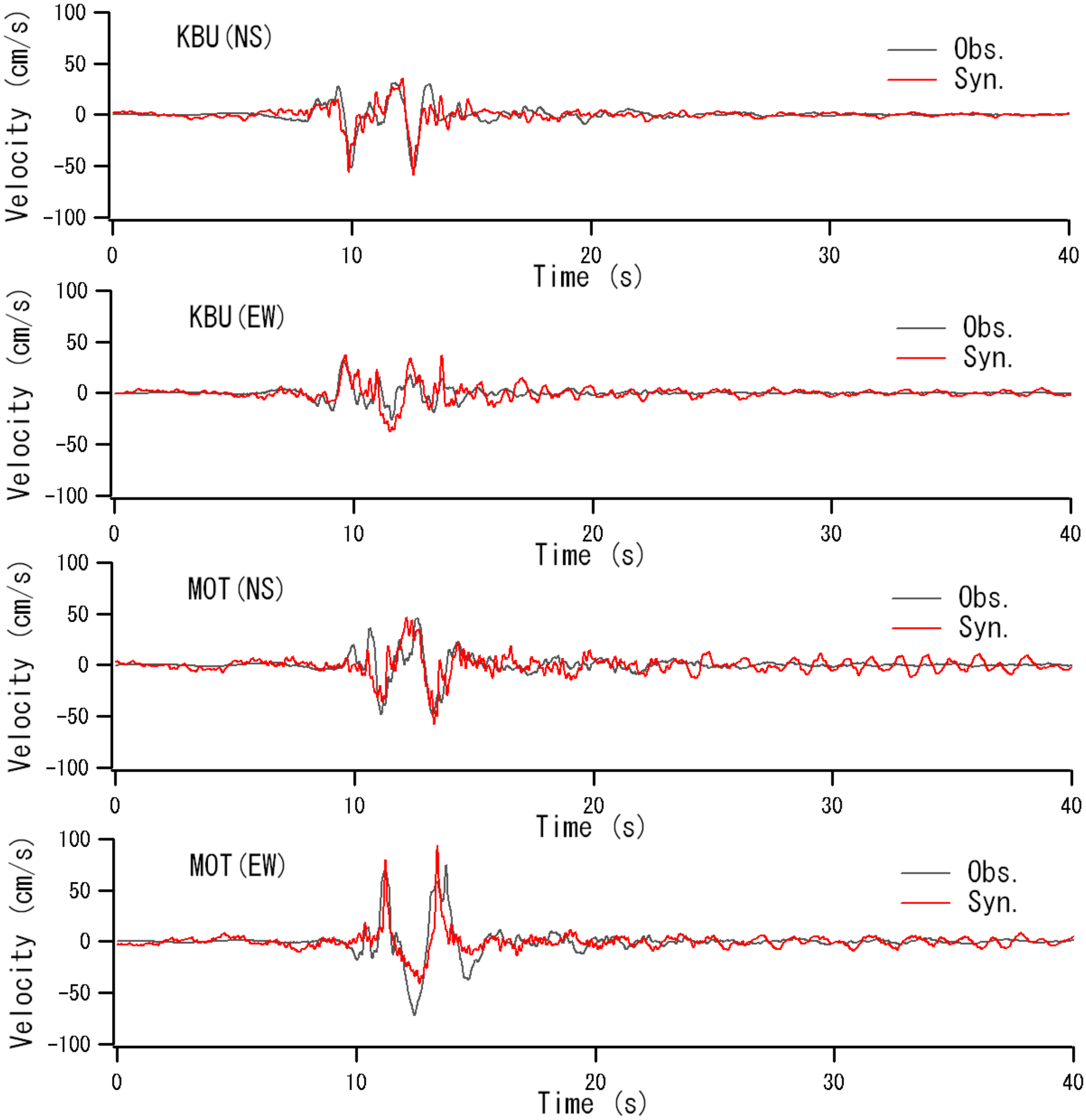

Figure 1 Observed and synthetic velocity waveforms at KBU and MOT

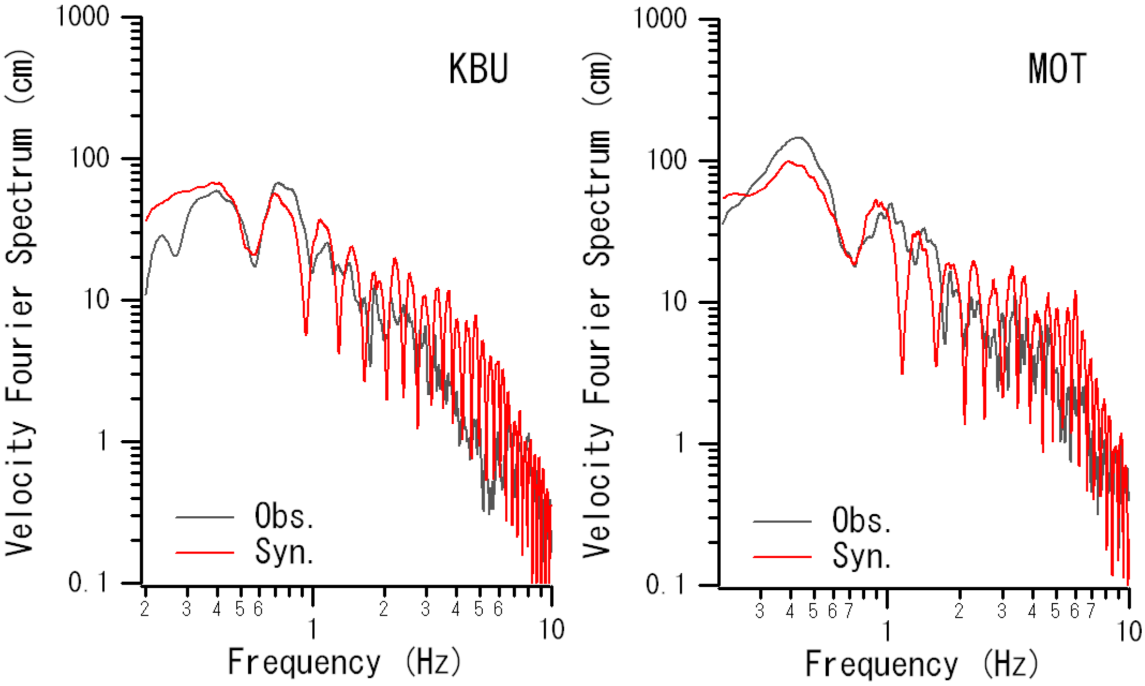

Figure 2 Observed and synthetic Fourier spectra at KBU and MOT
(composition for two horizontal components, parzen window 0.05Hz)

Characteristics of long-period motion in the Kathmandu Valley during the 2015 Gorkha Nepal earthquake sequence

*Michiko Shigefuji[1], Nobuo Takai[1], Subeg Bijukchhen[1], Masayoshi Ichiyanagi[1], Tsutomu Sasatani[1]

1.Hokkaido University

On 25 April 2015, a large M_W 7.8 earthquake occurred along the Himalayan front. The epicenter was near the Gorkha region, 80 km north-west of the Kathmandu Valley, and the rupture propagated eastward from the epicentral region passing through the Kathmandu Valley and reached Sindhupalchok region. The largest aftershock (M_W 7.3) occurred on 12 May 2015 at Sindhupalchok region, 74 km east of the Kathmandu. The Kathmandu Valley is formed by drying of a paleo-lake and consists of thick soft sediment below the center of city. Hence, the Kathmandu city has been damaged not only by near field earthquakes but also far field earthquakes in the past. As for the mainshock, there are 6 strong motion stations (one rock site and five sedimentary sites in the valley (Takai et al. 2016, Bhattarai et al. 2015, USGS 2015) that recorded the data. Long- period ground motions were recorded on sedimentary sites during the mainshock and aftershocks. We will examine the long-period (2-10 sec) motions in the Kathmandu Valley during the mainshock and aftershocks (M_W > 6).
Mainshock: The velocity waveforms observed at the rock site KTP show the typical velocity pulse ground motions (5 sec), and there are no clear later phase. The fault parallel component velocity waveform shows a double-sided pulse, while the fault normal and vertical components show a single-sided velocity pulse. The Kathmandu Valley is located at a very close distance (~10 km) to the rupture area and the estimated large slip areas exist near the valley (Galetzka et al. 2015). Therefore, the observed velocity pulses may be effected by this fault rapture process. The vertical component ground velocities at the sedimentary sites are nearly the same as that observed at the rock site KTP. On the contrary, the horizontal ground velocities at the sedimentary sites have a long duration with conspicuous long-period oscillations. We tried 1-D amplification simulation for sedimentary sites using with KTP record as input motion to examine the cause of this long period motion (Bijukchhen et al. 2016) and we could know the importance of examining the effect of 2,3-D valley basement structure.
Largest Aftershock: We could recognize peaks around 0.1 Hz in the Fourier velocity spectra for all stations. Therefor we applied low-pass filter (0.2 Hz) for the velocity waveforms and plotted particle motion. Including rock site KTP, we observed retrograde motion just after initial S-wave motion from these particle motion. These motions should have been controlled by propagation of Rayleigh wave; the Rayleigh waves were also observed in the other shallow aftershocks (Δ~80 km). We examined this phenomenon by the Discrete Wave Number method (Takeo, 1985) with 1-D velocity structure (Monsalve et al. 2006) and GCMT source mechanism. The simulated waveforms have good fitness with observed records and we could grasp the excitation of Rayleigh waves.
In this examination, we recognize the difference in excitation and propagation of long-period ground motions during the mains hock and aftershocks. We will study the excitation and propagation of surface wave in the Kathmandu basin in detail.

Keywords: The 2015 Gorkha Nepal earthquake sequence, Kathmandu Valley, Strong motion records, Long-period motion

Simulation of long-period ground motions in the Kathmandu basin during the 2015 Gorkha, Nepal, earthquake

*Hisahiko Kubo[1], Yadab Prasad Dhakal[1], Wataru Suzuki[1], Takashi Kunugi[1], Shin Aoi[1], Hiroyuki Fujiwara[1]

1.National Research Institute for Earth Science and Disaster Prevention

The 2015 Gorkha earthquake (M_w 7.9) occurred in the central Nepal at 06:56 on 25 April 2015 (UTC), and caused extensive damage to the Nepal society. During the 2015 Gorkha earthquake, strong ground motions with predominant components at 4–5 s period were observed in the Kathmandu basin (e.g. Galetzka et al. 2015; Takai et al. 2016). The waveform observations inside and outside the Kathmandu basin indicated that the characteristic long-period ground motions were caused by both effects of the source and Kathmandu basin. In order to investigate how well the long-period ground motions can be reproduced by available source and structure models, we carried out the waveform simulation in long period (> 4 s) at KATNP site located in the Kathmandu basin using the source model obtained by the joint source inversion and the estimated 1D velocity structure model for the Kathmandu basin.
The source process of the 2015 Gorkha earthquake was estimated by the fully Bayesian multiple-time-window source inversion (Kubo et al. 2016) with jointly using near-field waveforms, teleseismic waveforms, and geodetic data. The estimated seismic moment and maximum slip are 7.5×10^{20} Nm (M_w 7.9) and 7.3 m, respectively. The total source duration is approximately 50 s. The derived source model has a unilateral rupture towards east and a large slip area north of Kathmandu with the maximum slip.
The 1D deep subsurface velocity structure beneath KATNP was constructed by a trial-and-error process to reproduce the peak period on the long-period side of the horizontal-to-vertical spectral ratios of coda waves from eight aftershock recordings. The available geological and geophysical information were also utilized in this process. In this basin structure model, the thickness of low-velocity (Vs < 500 m/s) layers is approximately 460 m.
Using the derived source model of the 2015 Gorkha earthquake and the structure model of the Kathmandu basin, we carried out the simulation of the long-period ground motions during the 2015 Gorkha earthquake. The simulation demonstrated that the major features of the observed waveforms can be reproduced by our source and basin structure models.
[Acknowledgments] The high-rate GPS data provided by the Department of Mines and Geology, Tribhuvan University, and California Institute of Technology, and the strong motion data observed by the USGS were used in this study.

Keywords: Long-period ground motions, The 2015 Gorkha earthquake, The Kathmandu basin, Waveform simulation

Detection of nonlinear site response using the main shock and its aftershocks of the 2015 Gorkha, Nepal Earthquake recorded at the DMG site of the Kathmandu Valley, Nepal

*Mukunda Bhattarai[1], Lok Bijaya Adhikari[1], Umesh Prasad Gautam[1], Bharat Prasad Koirala[1], Chintan Timsina[1], Toshiaki Yokoi[2], Takumi Hayashida[2], Laurent Bollinger[3]

1.Department of Mines and Geology, Ministry of Industry, Nepal , 2.International Institute of Seismology and Earthquake Engineering, Building Research Institute,Japan, 3.Departement Analyse Surveillance de l'Environnement, Commissariat Energie Atomique, France

We have tested the occurrence of non-linear behavior of soil at the DMG site using the accelerograms of the main shock and its aftershocks during the 2015 Gorkha, Nepal Earthquake. The DMG accelerometric station is installed on the surface at the concrete slab of the single-storey office building in the central part of the Kathmandu Valley filled by sediments. We calculated the horizontal to vertical spectral ratios of S-waves part of the earthquake records (S-H/V) which is expected to provide information about the ground response. Then we calculate the degree of non-linearity (NDL) (Noguchi and Sasatani 2008) for the main shock and its 5 aftershocks in the frequency range from 1 Hz to 10 Hz. It is found that DNL of the main shock record clearly different from those of the aftershocks records. The PGA-DNL plot shows that the main shock runs off from the trend formed by the aftershock records.
Based on the above study we guess that non-linear behavior took place during the main shock of the 2015 Gorkha, Nepal Earthquake.

Keywords: Non-linear site effect, Degree of non-linearity, Gorkha earthquake, Kathmandu Valley

Relationship between Irregularity of Boundary of Subsurface Geology and Spatial Variation in Peak Periods of Horizontal to Vertical Spectral Ratio of Microtremors -A Study Based on Numerical Simulations-

*Kentaro Motoki[1], Tetsushi Watanabe[1], Kenichi Kato[1]

1.Kobori Research Complex

Earthquake motions on an irregularly layered subsurface geology (hereafter irregular site) sometimes show a higher amplification than on a stratified media (hereafter flat site) due to, for example, a focusing effect of seismic waves. An exploration of depth distribution of geological boundary is necessary for a reliable estimation of amplification factor at an irregular site, but it is too costly to make such a survey at every site in practice. Before a detail survey, a simple method to sort out irregular site from flat site is desired for insufficient geological information sites. Focusing on spatial variation in peak periods of horizontal to vertical spectral ratios (hereafter HVSRs) of microtremors, we showed in Motoki et al.(2012) that the values of coefficients of variation (hereafter CVs) were obviously separated between irregular sites and flat sites. In this report, we performed 2 investigations using numerical simulations with respect to a relationship between CVs and irregularity of subsurface geology.
First, in order to reveal what kind of parameters of subsurface geological model affected amplitude of CVs, we analyzed a sensitivity for CVs by numerical simulation with various parameters. The basic geological model was constructed based on results of drilling method at Nabari site where mobile microtremor measurements were also conducted. CVs of simulated motions with the basic model are almost consistent with the CVs by the observations. We found out that slope angles and horizontal sizes of irregularity affected amplitudes and inflection distances of CVs.
Second, we directly compare CVs to irregularity of subsurface geology, using results of simulated microtremors and geological models. For a comparison, we converted CVs to a power spectral density (hereafter PSD) via a semivariogram, which were frequently used in geostatistics. The PSD estimated from the CVs showed a good agreement with the PSD calculated from geological model in the wave number range corresponding to interstation distances to estimate the CVs. Note that we can say CVs reflect irregularity of subsurface geology.
We evaluated the difference of CVs by fluctuating irregularity of subsurface geology through numerical simulations. Consequently, we found that CVs can be an index of the irregularity, and we will suggest a procedure and a threshold in future works.

Keywords: Microtremors, Peak period of H/V, Spatial variation, Coefficients of variation, Power spectral density

Estimation of S-wave velocity structures of an irregular ground using H/V spectral ratio ~Case study in the middle coast of Miyazaki prefecture~

*Kyosuke Okamoto[1], Seiji Tsuno[1], Masahiro Korenaga[1]

1.Railway Technical Research Institute

S-wave velocity structures have been estimated from dispersion curves of phase velocity, H/V spectral ratios, etc., using microtremor exploration technique. However the estimations are originally based on the assumption that underground structures have stratified horizontally. So, if structures have irregular, e.g., layers incline or discontinue, the structures estimated under the assumption of horizontal stratification have errors to some extent due to perturbation of wave filed at the irregular. On the other hand, it has been known that seismic waves are likely to be amplified at the irregular structures since the various seismic waves interfere with each other. So, accurate estimation of the irregular structures is needed for disaster prevention. Seismic reflection and boring surveys are powerful tools to estimate the irregular structures since boundaries of the structure are directly imaged. However sometimes they have difficulties in cost and space for their application, especially surveys of a wide range of areas are limited. Here, we focus on H/V spectral ratios, which are relatively easy to measure a wide range of areas with a small budget, to estimate a dipping structure.

In this study, we applied microtremor explorations and observed earthquake ground motions (from Sep. to Nov., 2015) along Miyazaki maglev test line (Railway Technical Research Institute), where an irregular structure has been estimated by a preceding study, to examine the applicability of microtremor expirations to irregular structures. The microtremor explorations and the observations of earthquake ground motions were conducted at 8 points with about 290m intervals along a 2km survey line, whose center is the irregular point. We estimated S-wave velocity structures at each observation points by the SPAC method, and confirmed that the dipping structure exists at the location pointed out by the preceding study. We validated the structures estimated at each observation points by checking the similarity of the converted seismic waves on the basement. We also confirmed that the theoretical H/V spectral ratios of the observation points calculated by the multiple reflection theory agree with the observed H/V spectral ratios well. It suggests that H/V spectral ratios can illuminate the dipping structure. However, the theoretical and observed H/V spectral ratios disagree with largely each other around the edges of the dipping structure. One of the causes of this disagreement is that a complex wave filed is produced by reflecting waves, higher modes of surface waves, etc., at the dipping structure, and it cannot be accounted by the assumption of horizontal stratification.

To examine the original locations of the disturbance in the wave field, we synthesized the wave field using a numerical simulation using the estimated structure model. We divided the synthesized wave at the edges of the dipping structure into surface wave and the others (reflections, refractions and etc.), then, we calculated the original locations of the latter waves based on the method of back propagation. As a result, it was revealed that part of the dipping structure within one-wavelength from the issued receiver (here, the receiver at the edges) gives major effect in terms of the disturbance. We also confirmed that the H/V spectral ratio calculated using the divided surface wave agrees to the theoretical H/V spectral ratio, which is based on the assumption of horizontal stratification. It implies that the disturbance in wave fields (reflections, refractions, etc.) perturb the observed H/V spectral ratios.

In this study, we interpreted using a 2-D model. As a further discussion, it is necessary to consider 3-D effects.

Keywords: microtremor exploration, Earthquake ground motion, dipping structure

A Method of Estimating Incident Wave Considering Nonlinear Response of the Non-uniform Surface Ground

*Shotaro Yamada[1], Toshihiro Noda[2], Akira Asaoka[3], Yoshihiro Sawada[3]

1.Civil Engineering, Nagoya University, 2.Disaster Mitigation Research Center, Nagoya University, 3.Association for the Development of Earthquake Prediction

When a strong earthquake motion is the case, whether a seismometer is installed underground or on a ground surface, any information recorded through the seismometer should naturally reflect the influence of highly nonlinear mechanical behavior of a surface ground that usually exhibits non-uniform multi-layered system. In other words, every strong ground motion analysis cannot be performed without the use of soil mechanics that describes nonlinear mechanical behavior of a non-uniform surface ground system.

In recent years, the elasto-plastic finite deformation computation of a soil water coupled system[1)] is utilized for the analysis of surface ground behavior from deformation to failure including soil liquefaction that occurs during/after a strong 'quake. In this research, a method of estimating input earthquake motion at an engineering base surface is newly presented from the records of seismometer at the basement that should reflect nonlinear mechanical behavior of a non-uniform multi-layered surface ground.

In the presented method, the existence of a semi-infinite purely elastic ground is assumed blow the so-called "horizontal engineering base surface" along which viscous boundary[2), 3)] is introduced at the bottom of a surface ground system. The earthquake motion is input at the bottom of surface ground through the viscous boundary. Let E be the upward transmitting wave, while F, the downward wave. In the usual "viscous boundary analysis", the E is assumed at the viscous boundary as an input data and the whole surface ground motion is solved. As the results, the E+F is obtained at viscous boundary. Therefore, in usual computation, by giving E, at a viscous boundary, E+F is calculated at any point on the boundary. This E+F will be recorded if a seismometer is installed at the engineering base surface. However, the input data E is always to be assumed. The recorded and then observed E+F cannot be the 2E, because F includes every influence of both nonlinear mechanical behavior of ground motion and non-uniform geometrical shape of a multi-layered surface ground system. In this research, a method is newly proposed of calculating E by the use of observed E+F as an input data.

It is naturally considered that incident wave E should be uniformly distributed on an engineering base surface. This constrained motion at the bottom of surface ground is introduced through a "method of Lagrange multiplier", in which Lagrange multiplier is to give the constrained force. Therefore, E is solved, from time to time, by calculating Lagrange multipliers.

For the verification of the method, the need of measurement of E+F at many locations on/in the surface ground is particularly emphasized in this research.

References

1) Noda, T., Asaoka, A. and Nakano, M. (2008): Soil-water coupled finite deformation analysis based on a rate-type equation of motion incorporating the SYS Cam-slay model, *Soils and Foundations*, 45(6), 771-790.

2) Lysmer, J. and R., L., Kuhleemeyer (1969): Finite dynamic model for infinite media, *ASCE*, EM4, 859-877.

3) Noda, T., Takeuchi, H., Nakai, K. and Asaoka, A.(2009):Co-seismic and post-seismic behavior of an alternately layered sand-clay ground and embankment system accompanied by soil disturbance, *Soils and Foundations*, 49(5), 739-756.

Keywords: incident wave, observed wave, engineering base surface, surface ground, nonlinear analysis, viscous boundary

Numerical realization of surface waves and assessing their influence on liquefaction using 2D effective stress analysis

*Kentaro Nakai[1], Toshihiro Noda[2], Akira Asaoka[3], Sho Ozaki[1]

1.Graduate School of Engineering, Nagoya University, 2.Disaster Mitigation Research Center, Nagoya University, 3.Association for the development of earthquake prediction

One of the important characteristic of surface waves is that distance attenuation is small compared with P-wave and S-wave. Therefore, it can propagate to hundreds of kilometers away from epicenter, and leads to a post-motion phenomenon of relatively large continued tremors even after the primary motion has ended. Moreover, complex interference between the surface waves and the body wave causes extensive and localized seismic damage. However, the influence of surface waves on liquefaction damage is not fully understood yet. This report tries to reproduce surface waves and assess its influence on liquefaction with the use of 2D elasto-plastic seismic response analysis considering the effect of irregularly shaped bedrock. The analysis code employed in this report was the soil-water coupled finite deformation analysis code GEOASIA[2)], which incorporates an elasto-plastic constitutive model[1)] that allows description of the behavior of soils ranging from sand through intermediate soils to clay under the same theoretical framework.
The ground model was prepared with its height 100m and width 30,000m. Bedrock was assumed to be inclined at extreme left side of the ground. Stratum organization was assumed to be Pleistocene layer in deep part, above which was a sensitive soft clayey layer, followed by a loose sandy layer with reference to Urayasu ground[3)]. The hydraulic boundary was set that the ground surface coincided with water level was set up as water pressure equal zero. The bottom face and the two lateral faces were assumed to be undrained boundaries. The seismic wave that was observed at a depth of about G.L. -36 m at Shinagawa observation point of the Tokyo Bureau of Port and Harbor (see Fig.1 (a)) was input as a 2E-wave in the horizontal direction only at the bottom face beneath the inclined bedrock area. In addition to establishing simple shear deformation boundaries at the two lateral ends of the boundaries, a viscous boundary equivalent to Vs=400 m/s was set up at the bottom face of both excitation and non-excitation area. Fig.1 (b) illustrates the velocity vector distribution 100 sec after the earthquake occurrence. Surface waves are generated at the base end section of the inclination which shows orbit in a counterclockwise direction with ongoing wave propagation to the right-hand side. Fig.1 (d) illustrates the acceleration responses at locations A, B and C. Location A sited left side of inclined bedrock shows smaller acceleration compared with location B and doesn’t generate vertical motion. On the other hand for location B, in addition to the generation of vertical motion, duration and maximum acceleration are enlarged for horizontal motion caused by the propagation of surface waves. Moreover, location C sited 20,000km away from excitation area still observed acceleration response, although the maximum amplitude is around 30gal. This seismic motion can be regarded as surface waves so that the similar acceleration response can be observed at location C’. Fourier amplitude of the surface waves is dominant at slightly long-period around 1.7 sec. Fig.1 (c) illustrates mean effective stress reduction ratio at each location. Although the reduction ratio at location A didn’t increase so much, location B gradually increases even after the primary motion and finally reaches to 95% which indicates liquefaction. Gradual increase was caused by the complex interference between the surface waves and the body wave. Moreover, location C is also gradually increased to the extent of 60% even the observed seismic motion is not so large. This result indicates that the location C has a risk of delayed-liquefaction damage with additional aftershock excitations.
1) Asaoka, A. et al. (2002): An elasto-plastic description…, S&F, 42(5), 47-57.

2) Noda, T. et al. (2008): Soil-water coupled ⋯, S&F, 48(6), 771-790.
3) Nakai,K. et al. (2014): Liquefaction damage expansion⋯, JGUM, SSS23-19.

Keywords: surface wave, liquefaction, irregularly shaped bedrodk, effective stress analysis

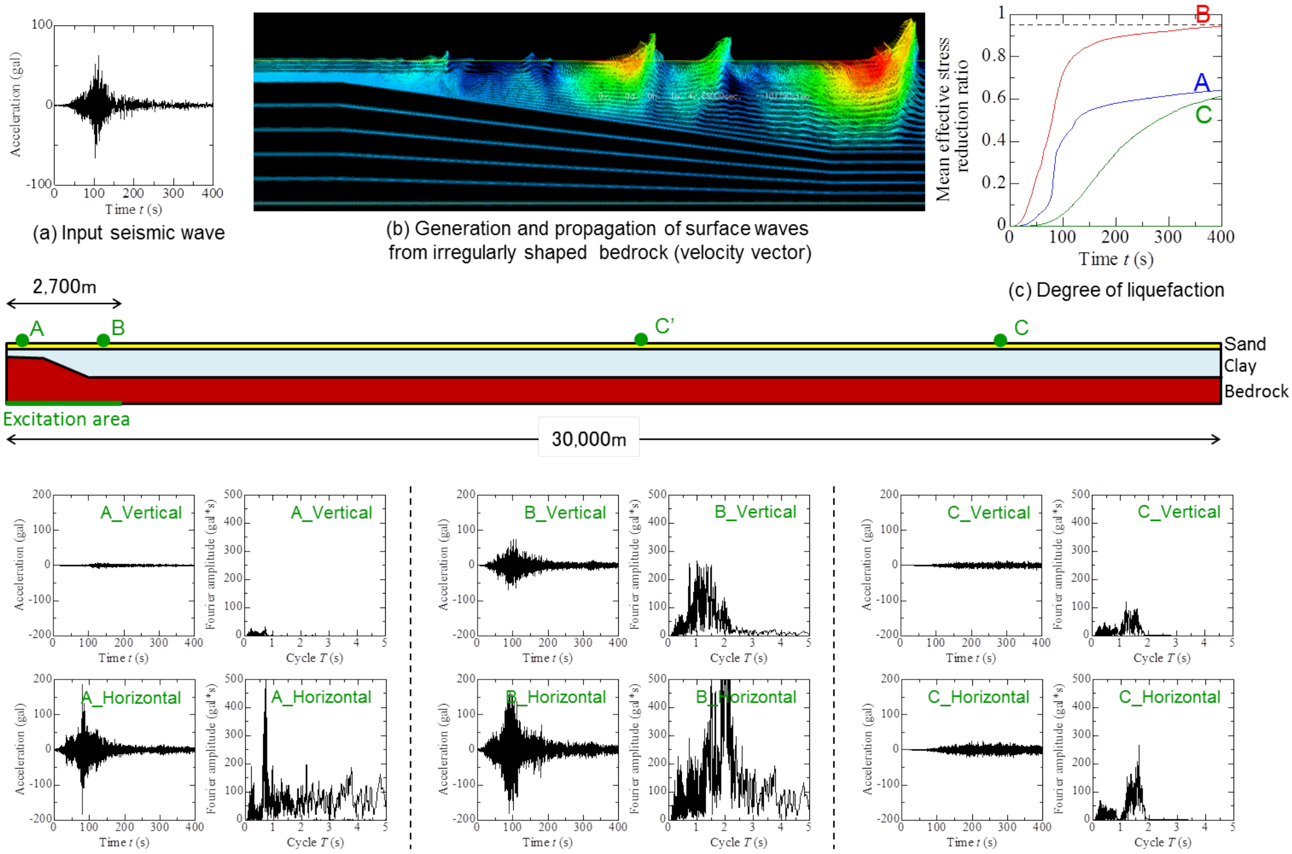

(a) Input seismic wave
(b) Generation and propagation of surface waves from irregularly shaped bedrock (velocity vector)
(c) Degree of liquefaction

(d) Acceleration and Fourier amplitude at different subsurface place

Earthquake Fatalities Mapping for the Eastern Asia Earthquake and Volcanic Hazards Information Map

*Masayuki Yoshimi[1], Yuzo Ishikawa[1], Shinji Takarada[1], Jeol Bandibas[1], Tadashi Maruyama[1], DAN MATSUMOTO[1], Takashi AZUMA[1], Ryuta FURUKAWA[1], Akira Takada[1], Yasuto Kuwahara[1], Eikichi Tsukuda[1]

1.Geological Survey of Japan, AIST

The Eastern Asia Earthquake and Volcanic Hazards Information Map is published in May 2016. This map illustrates geology and tectonics, active faults, earthquakes hypocenters and source areas, fatalities of major earthquakes, tsunami hazards, distribution of volcanoes, calderas, pyroclastic falls and ignimbrites, and fatalities of major volcanic events. We believe that this hazards information map will provide useful information for earthquake, tsunami, and volcanic disaster mitigation efforts.
Earthquake fatalities map is one of the major contents, which has been compiled to facilitate visual understanding of earthquake disasters in terms of their number of fatalities (deaths) and the main causes of deaths. Major disastrous earthquakes in terms of number of fatalities are selected in each country or region: all the recent (after 1850) events with fatalities more than 1,000 (hereafter, F1000 event) are included; for a country with less than three F1000 events, two F100-F10 events are added; for a country with no F1000 events, up to two F100 events or one worst earthquake with fatalities are added. The number of fatalities is categorized by five causes; structure (building) damage, tsunami, landslide, fire, and others (related death), when possible. It is important to understand that an earthquake and ground motions do not directly kill people, but vulnerable structures, fire, landslide, or tsunami do. The number of fatalities is mainly based on the Significant Earthquake Database (NGDC/WDS) provided by NOAA, and indivisual reports of each earthquake, if any.
The contents of the Information Map are planning to be implemented on the online hazard information system (http://ccop-geoinfo.org/G-EVER). We are going to collect more data or reports to make the map more reliable.

Keywords: Eastern Asia, disastrous earthquake, number of fatalities

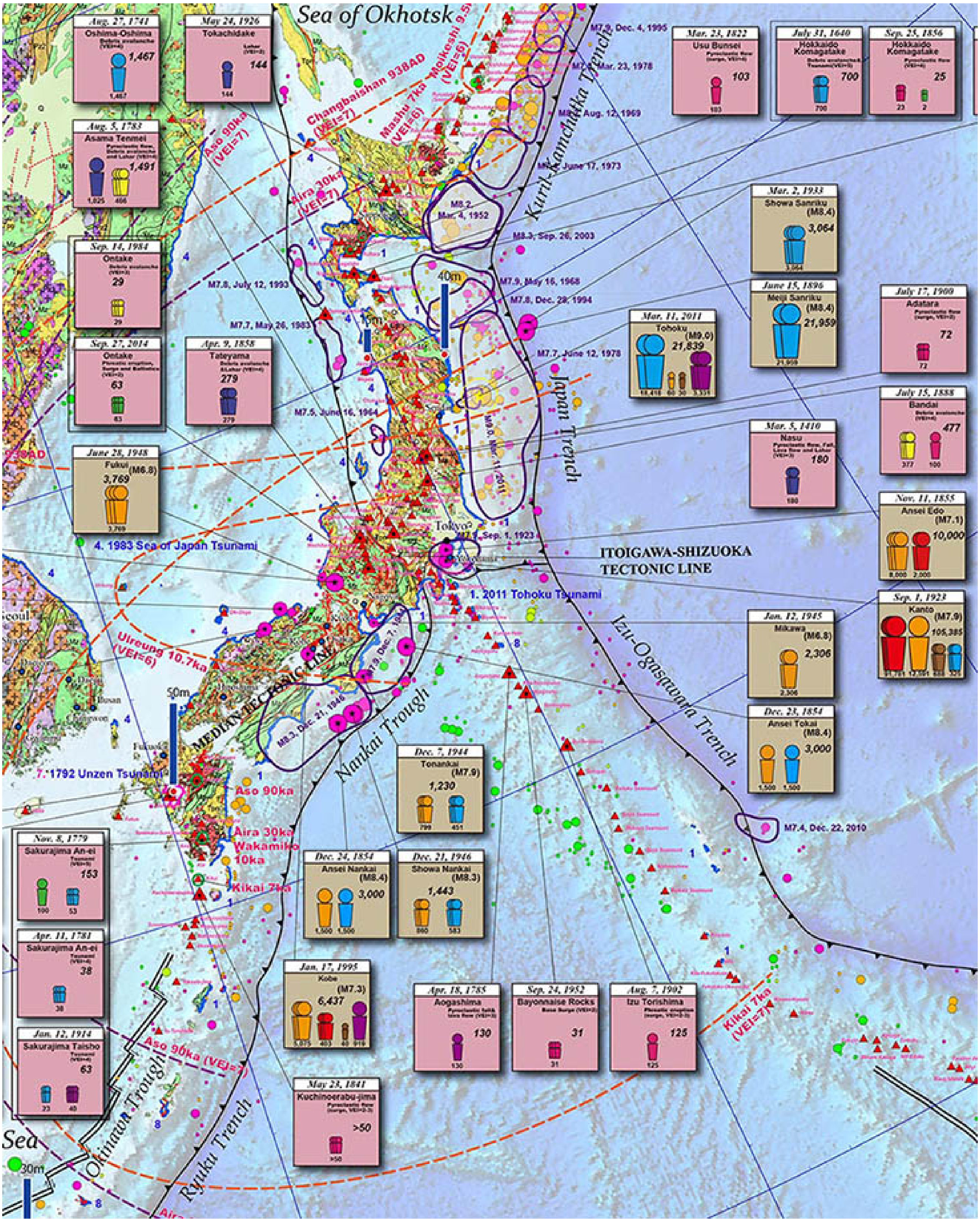
Sea of Okhotsk
Kuril-Kamchatka Trench
Japan Trench
Izu-Ogasawara Trench
Nankai Trough
Okinawa Trough
Ryukyu Trench
MEDIAN TECTONIC LINE
ITOIGAWA-SHIZUOKA TECTONIC LINE
Tokyo
Seoul
Busan
Changbaishan 938AD (VEI=7)
Mashu 7ka (VEI=6)
Aso 90ka (VEI=7)
Aira 30ka (VEI=7)
Ulreung 10.7ka (VEI=6)
Kikai 7ka (VEI=7)
Aso 90ka
Aira 30ka
Wakamiko 10ka
Kikai 7ka
Aso 90ka (VEI=7)
1. 2011 Tohoku Tsunami
4. 1983 Sea of Japan Tsunami
7. 1792 Unzen Tsunami
M7.9, Dec. 4, 1995
M7.7, Mar. 23, 1978
M8.2, Aug. 12, 1969
M7.8, June 17, 1973
M8.2 Mar. 4, 1952
M8.3, Sep. 26, 2003
M7.9, May 16, 1968
M7.8, Dec. 28, 1994
M7.7, June 12, 1978
M7.8, July 12, 1993
M7.7, May 26, 1983
M7.5, June 16, 1964
M9.0, Mar. 11, 2011
M7.9, Sep. 1, 1923
M8.3, Dec. 21, 1946
M7.4, Dec. 22, 2010
40m
50m
30m
Aug. 27, 1741 Oshima-Oshima 1,467
May 24, 1926 Tokachidake 144
Aug. 5, 1783 Asama Tenmei 1,491
Sep. 14, 1984 Ontake 29
Sep. 27, 2014 Ontake 63
Apr. 9, 1858 Tateyama 279
June 28, 1948 Fukui (M6.8) 3,769
Mar. 23, 1822 Usu Bunsei 103
July 31, 1640 Hokkaido Komagatake 700
Sep. 25, 1856 Hokkaido Komagatake 25
Mar. 2, 1933 Showa Sanriku (M8.4) 3,064
June 15, 1896 Meiji Sanriku (M8.4) 21,959
Mar. 11, 2011 Tohoku (M9.0) 21,839
July 17, 1900 Adatara 72
July 15, 1888 Bandai 477
Mar. 5, 1410 Nasu 180
Nov. 11, 1855 Ansei Edo (M7.1) 10,000
Sep. 1, 1923 Kanto (M7.9) 105,385
Jan. 12, 1945 Mikawa (M6.8) 2,306
Dec. 23, 1854 Ansei Tokai (M8.4) 3,000
Dec. 7, 1944 Tonankai (M7.9) 1,230
Dec. 24, 1854 Ansei Nankai (M8.4) 3,000
Dec. 21, 1946 Showa Nankai (M8.3) 1,443
Jan. 17, 1995 Kobe (M7.3) 6,437
Apr. 18, 1785 Aogashima 130
Sep. 24, 1952 Bayonnaise Rocks 31
Aug. 7, 1902 Izu Torishima 125
May 23, 1841 Kuchinoerabu-jima >50
Nov. 8, 1779 Sakurajima An-ei 153
Apr. 11, 1781 Sakurajima An-ei 38
Jan. 12, 1914 Sakurajima Taisho 63

Age-dependent Mortality in the 2011 East Japan Eartuquake -Further Revision of Traditional Mortality at Attack by Tsunami

*Yutaka Ohta[1], Maki Koyama[2], Tomoko Shigaki[3]

1.Tono Research Institute of Earthquake Science, 2.River Basin Research Center Gifu University, 3.Institute of Erderly Housing Science

1. Preface
This paper reports a further development of known age-band specific mortality equation at attack by a tsunami. The equation in a certain age-bound has been written as
Mortality (%) =Number of deaths / Number of people concerned (1).
The equation looks therefore apparently simple enough. But, the reality is different from what we see in the equation, since the equation itself gives no special constraint. Incidentally, there come two essential issues to keep in mind at application.
The first one gives very low mortality for infants and children in case when a straight application of the equation is made to the 2011 giant tsunami, and on the contrary it gives very high mortality for aged people, which seems far illogical.
The second issue requiring careful treatment is how to fix the appropriate population concerned. Employing either prefectural or municipal census data with age-specific population by 5-year intervals is very convenient because of its easy accessibility, but we should be careful on whether or not those data are responsible for the real number of population attacked by a tsunami. As has already been criticized by Sawai[1)], we should keep in mind of regulation of population to be suited to have direct comparisons in one event or in plural numbers of natural disasters as of earthquakes, tsunamis and, etc.
2. Methodology to overcome the above-stated two serious issues
In order to overcome the first issue we applied the Ozaki's method[2)] with a little modification. The essential point in his method is to give a special weight to a comparison of the mortality attacked by the natural disaster as tsunami, with that in one ordinary year during which no devastating disaster attacks. Thus we can get rid of any misunderstandings[3)].
To overcome the second issue we finally adopted the outstanding outcomes by Koyama and her colleagues[4)] who succeeded counting of residents in the area inundated by the tsunami and in the area where their living houses were swept away. Since we have known by Hatori's work[5)] that the residents killed are mostly living in the swept-away houses, we placed higher priority on the number of residents living in the swept-away area.
3. Concluding Remarks
The finally obtained are summarized as in the followings.
1) For the mortality evaluation by the attack of tsunami, it is necessary to have a comparative study with the mortality in one ordinary year with no disasters.
2) Reasonable population at the mortality evaluation by tsunami is to count the number of occupants living in the swept-away houses by the tsunami.
3) We can evaluate the severity of mortality by tsunami just by ratio with one ordinary year with no significant disasters, and we are easy to understand that infants' mortality at attack by tsunami is far severer than that in one ordinary year.
4) In spite of the fact as in 3), in a few areas nearby Kamaishi city in Iwate Pref., we found the mortalities are relatively smaller, which suggests the effectiveness of special training frequently guided by Katada[6)].
5) We have recognized a certain positive correlation between the derived

mortalities and tsunami heights.

References

1) Ozaki, kousei no shihyou, 59, 2012 (in Japanese).
2) Ohta, Koyama and Shigaki, Mortality in the 2011 East Japan Earthquake (2~6). JpGU Meeting, 2013-15.
3) Sawai, M., Who is vulnerable during tsunamis? , 1-18, 2012, ESCAP Spec. Rep.
4) Koyama et al, Municipality’s mortality rate according to Inundation level and age on the 2011 Tohoku earthquake, Earthq. Engr., Japan Civil Engr., 2012.
5) Hatori, Damage rate of Residential Houses by a Tsunami, BERI, 59, 1984.
6) Katada; Hito ga shinanai bousai 2012, Shueisya.

Keywords: East Japan Earthquake, Tsunami, Mortality, Critical Revision